PROCEEDINGS OF SPIE

SPIEDigitalLibrary.org/conference-proceedings-of-spie

Photosensivity of heterostructures produced by aerosol deposition of ZnMgO thin films on Si substrates

Morari, Vadim, Monaico, Eduard, Rusu, Emil, Leistner, Karin, Nielsch, Kornelius, et al.

Vadim Morari, Eduard Monaico, Emil Rusu, Karin Leistner, Kornelius Nielsch, V. V. Ursaki, I. M. Tighineanu, "Photosensivity of heterostructures produced by aerosol deposition of ZnMgO thin films on Si substrates," Proc. SPIE 11718, Advanced Topics in Optoelectronics, Microelectronics and Nanotechnologies X, 1171818 (31 December 2020); doi: 10.1117/12.2571189

SPIE.

Event: Advanced Topics in Optoelectronics, Microelectronics and Nanotechnologies 2020, 2020, Online Only

Photosensivity of heterostructures produced by aerosol deposition of ZnMgO thin films on Si substrates

VadimMorari [1)*], Eduard Monaico [2)], Emil Rusu [1)], Karin Leistner [3)], Kornelius Nielsch [3)], V. V. Ursaki [2)] and I. M. Tiginyanu [2)]

[1)] ,,D.Ghitu" Institute of Electronic Engineering and Nanotechnologies, Chisinau MD-2028, Republic of Moldova

[2)] National Center for Materials Study and Testing, Technical University of Moldova, Chisinau MD-2004, Moldova

[3)] Leibniz Institute for Solid State and Materials Research of Dresden (IFW Dresden), Institute for Metallic Materials (IMW), 01069 Dresden, Germany

* Laboratory of Nanotechnology, Tel: +373 22739048, e-mail: *vadimmorari2018@gmail.com*

ABSTRACT

ZnMgO thin films were prepared on Si substrates by aerosol deposition method using zinc acetate and magnesium acetate as precursors. The obtained films were investigated by scanning electron microscopy (SEM), energy dispersive x-ray (EDX) and X-Ray Diffraction (XRD) analysis. SEM and EDX investigations showed that the produced thin films are homogeneous from the point of view of morphology and composition. The investigation of photosensitivity demonstrated that the heterostructures of ZnMgO thin films deposited on Si substrates are sensitive in a wide spectral range from ultraviolet (UV) to infrared (IR) radiation, with a highest sensitivity in the UV region.

Keywords: ZnO, ZnMgO, UV irradiation, photocurrent, photosensitivity.

1. INTRODUCTION

ZnMgO solid solutions system presents interest due to possibilities to tailor many important physical properties by varying their composition. This alloy system covers a wide ultraviolet (UV) spectral range between the direct bandgaps of 3.36 eV for ZnO and 7.8 eV for MgO at room temperature, therefore being very attractive for short-wavelength optical applications such as UV detectors [1-3] and light emitters [4-6]. The $Zn_{1-x}Mg_xO$ system [7,8] provides the possibility to model the optical, luminescent and photoelectric properties in a wide spectral range, by adjusting the composition in the system (x-parameter value). Devices for short wavelengths UV-A (320-400 nm), UV-B (280-320 nm) and UV-C (200-280 nm) radiation can be produced by changing the composition [9,10]. Nanostructuring of these materials, particularly the production of nanostructured films, is an additional element for modeling specific properties.Various techniques have been used for preparation of ZnMgO films such as pulsed laser deposition (PLD) [11], plasma-enhanced atomic layer deposition (PE-ALD) [12], hydrothermal [13], chemical bath deposition (CBD) [14], radio-frequency-plasma assisted molecular beam epitaxy (RF-MBE) [15-18], DC [19, 20] and RF [21-23] magnetron sputtering, chemical vapor deposition (CVD) [24], metal-organic chemical vapor deposition (MOCVD) [25, 26], aerosol deposition [27-31] and sol-gel spin coating [30, 32-35]. The aerosol deposition method has advantages of ensuring easy control and handling of chemicals and substrates, as well as excellent control over stoichiometry. It is suitable for fabrication of high quality large area thin film at faster rates and low cost due to non-vacuum equipment, low temperature processing, low defect density and low environmental impact. This method offers the possibility of depositing thin films in a fairly short time, easy doping and preparation of homogeneous films with good electrical and optical properties.

Advanced Topics in Optoelectronics, Microelectronics and Nanotechnologies X, edited by Marian Vladescu, Razvan Tamas, Ionica Cristea, Proc. of SPIE Vol. 11718, 1171818
 · doi: 10.1117/12.2571189

2. MATERIALS AND METHODS

2.1. Material preparation

Crystalline (100) p-type Si wafers «КДБ-10» doped with boron, specific electrical resistance 10 Ohm•cm^{-1} were used in our experiments. In order to obtain ZnMgO layers, the zinc acetate dehydrate ($Zn(CH_3CO_2)_2$•$2H_2O$) precursor with 99.999% purity and magnesium acetate tetrahydrate ($Mg(CH_3COO)_2$•$4H_2O$) precursor with purity ≥ 99% (both purchased from Sigma Aldrich) were dissolved in ethanol. The solutions for aerosol deposition were mixed in an ultrasonic bath for 30 minutes at a temperature of 50-60 °C to prepared $Zn_{1-x}Mg_xO$ films with x value of 0.2, 0.3, 0.4, and 0.6.

2.2. Aerosol deposition method

Aerosol deposition technology is one of the cheapest methods, which involves three major stages of the process: I - the preparation of precursor solutions; II - aerosol generation and transport; III - the film growth process. In the second stage, the distribution of the aerosol droplet size, determined by the aerosol transport mechanism, will establish the morphological characteristics of the final material produced. The last step determines whether the synthesized material is a powder or a film layer. In general, considering an experimental configuration, the synthesis parameters that are more relevant are the molarity of the precursor solution, the carrier gas flow rate and the synthesis temperature. The solvent in the precursor solution is chosen taking into account the solubility of the precursor compound and its physical properties, such as density and viscosity. The preferred choice is water or a mixture of water and alcohol, which will dissolve many inorganic salts (such as chlorides, some nitrates and fluorides). Organic salts will need organic solvents which, when selected correctly, could provide excellent precursor solutions, especially for thin film deposition processes. Therefore, the aerosol deposition method requires a substrate and a heater to maintain the surface temperature which is a critical factor in pyrolysis. The atomizer was placed at a distance L=18 cm above the heated Si substrate (*see Figure 1*). The distance L was chosen experimentally from the considerations of a uniform coverage on a larger surface. The temperature of the precursor solution during the aerosol deposition process was equal to 25 °C, while the substrate temperature was maintained at 500-550 °C by a temperature controller (БПРТ-1). The solution was inserted into a syringe, which then was mounted in a homemade device based on a stepper motor (Jova Solutions TIMS-0201™), being adjusted from the computer. The rate of deposition of the precursor solution was 0.33 ml/min and the deposition process lasted for 15 min.

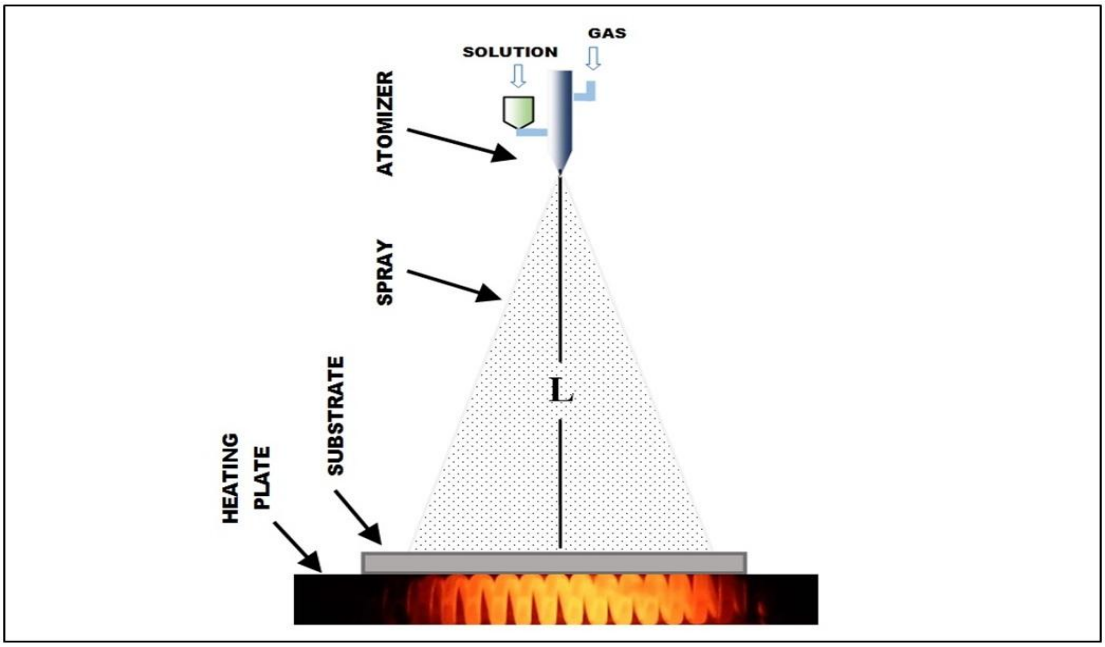

Figure 1.The method of aerosol deposition.

An aluminum contact was evaporated on the backside of Si substrate after deposition of the thin film. Upper contacts were fabricated from palladium trough a specially designed mask with 1.5 mm diameter in high vacuum with pre-heating of sample at temperature of 300 °C during 1 hour in the installation VUP-4.

3. RESULTS AND DISCUSSION

3.1. Morphology and chemical composition of $Zn_{1-x}Mg_xO$

The morphology and chemical composition analysis of the deposited layers was investigated using Scanning Electron Microscope (SEM) Zeiss LEO Gemini 1530 equipped with an Oxford Instruments INCA Energy EDX system operated at 20 kV. SEM images of $Zn_{1-x}Mg_xO$ film with 20% Mg concentration are presented in (*Figure 2*). The higher magnifications of SEM image reveal that the morphology is made of plates with a cabbage shape. Some nanoparticles with uniform size are observed in the top view as well as in the cross-section. The thickness of the deposited layer was estimated to be around 320 nm.

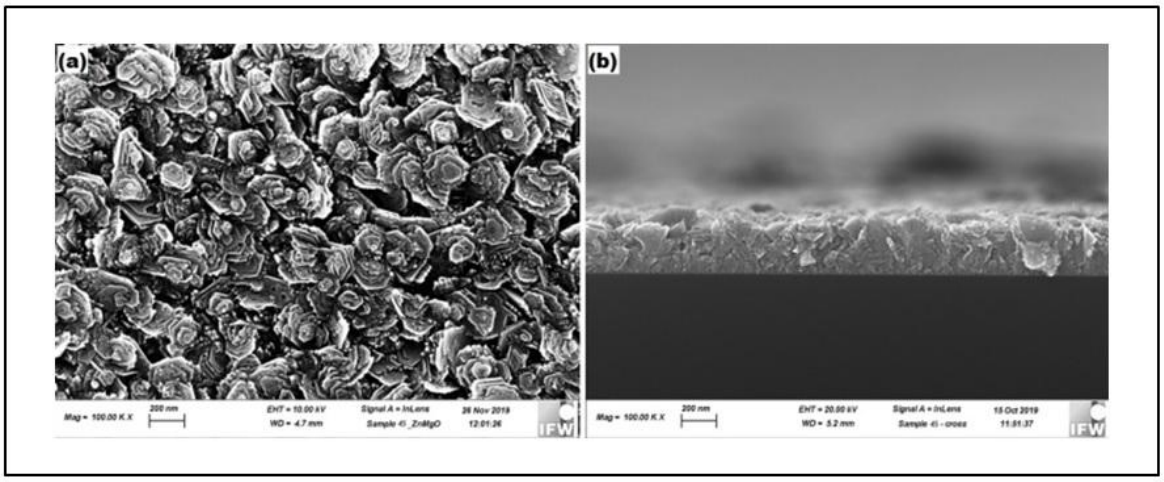

Figure 2. SEM images of a $Zn_{1-x}Mg_xO$ film with 20 % Mg.

The results of EDX analysis are presented in (*Table 1*).

Table 1. EDX chemical composition analysis of $Zn_{1-x}Mg_xO$ with 20 % Mg

Elements	Weight %	Atomic %
O	38.0	56.51
Mg	12.32	11.29
Zn	49.68	32.20
Totals	**100.00**	**100.00**

The increase of the Mg concentration to 40 % in the composition of the deposited film (*Table 2*) leads to visible changes in morphology (*see Figure 3*). While the thickness of the deposited layer remained unchanged, a higher density of dots with a larger diameter can be observed from a comparison of morphologies in (*Figure 2a)* and (*Figure 3a)*, which was assigned to the increase of the Mg concentration in the film.

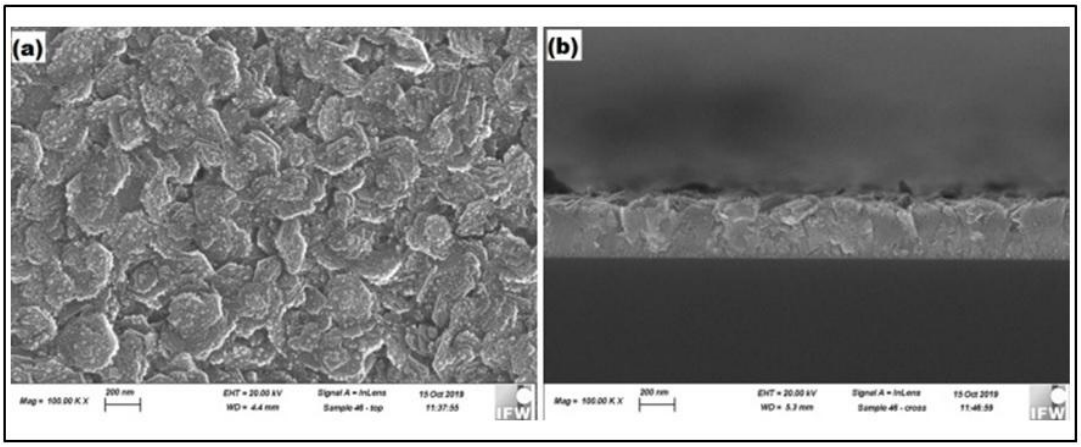

Figure 3. SEM images of a $Zn_{1-x}Mg_xO$ film with 40 % Mg.

Table 2. EDX chemical composition analysis of $Zn_{1-x}Mg_xO$ with 40 % Mg

Elements	Weight %	Atomic %
O	37.27	55.90
Mg	15.28	17.31
Zn	47.45	26.79
Totals	**100.00**	**100.00**

3.2. X-ray diffraction (XRD) analysis

The XRD measurements were carried out on a Rigaku Smart Lab X Ray Diffractometer using Cu K_α radiation (λ=0.15406 nm) are presented in (*Figure 4*). The identification of the phase was made by referring to the International Center for Diffraction Data – ICDD (PDF-2) database. The XRD peaks position of 33^o (100), 34.5^o (002), 36.5^o (101), 47.6^o (102) and 63^o (103) are the typical peaks for $Zn_{0.8}Mg_{0.2}O$. The peak around 42^o can be assigned to some trace of MgO, while the one at 44^o could be due to some Zn clusters.

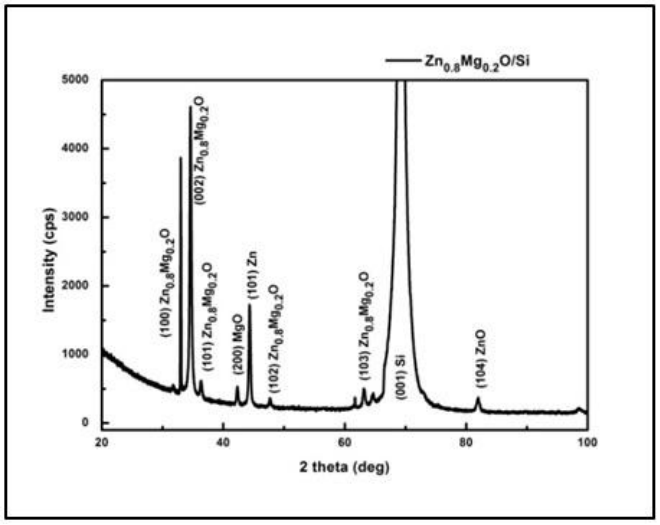

Figure 4. X-Ray Diffraction (XRD) analysis of a $Zn_{0.8}Mg_{0.2}O$ film annealed at 500 ^{o}C.

3.3. Photoresponse of a ZnMgO photodetector

The radiation from a Xenon lamp DKSS-150 was used to excite the photoconductivity in ZnMgO layers (*Figure 5*). Optical filters were used to select radiation from different spectral ranges (ultraviolet: 300–400 nm, power density at the sample surface 17.6 mW/cm^2; visible 400–700 nm, power density 25.5 mW/cm^2; and infrared 700–2500 nm, power density 134 mW/cm^2). The samples were illuminated with a focused beam of 5 mm in the diameter. The current through the samples was measured by means of a Keithley's Series 2400 Source Measure Unit. A mechanical shutter was used in the photoconductivity (PC) relaxation experiments. The signal from the Source Measure Unit was introduced in an IBM computer via IEEE-488 interface for further data processing. The measurements were performed at room temperature (300 K) in vacuum.

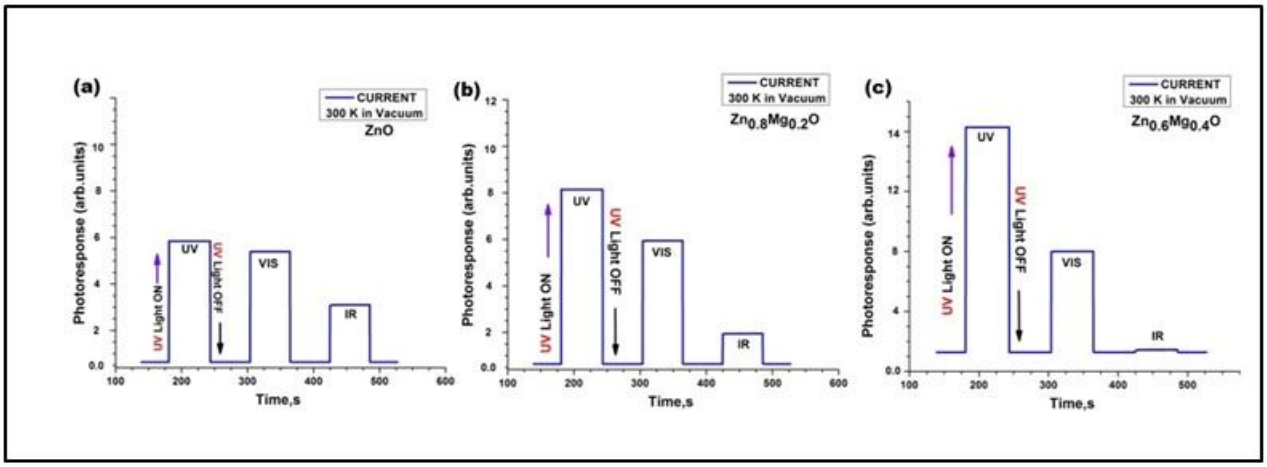

Figure 5. The photoresponse measured at 300 K in vacuum with radiation of different wavelengths for ZnO (a) and $Mg_xZn_{1-x}O$ films with x = 0.2 (b) and x = 0.4 (c) deposited on Si substrates.

The investigation of photosensitivity demonstrated that the heterostructures based on ZnMgO thin films deposited on Si substrates are sensitive in a wide spectral range from ultraviolet (UV) to infrared (IR) radiation, with a highest sensitivity in the UV region. While the ZnO film demonstrates a lower signal in the UV spectral region (*Figure 5 a*), the UV signal increases with increasing the Mg concentration (*Figure 5 b,c*).

3.4. Optical absorption spectra of ZnO-ZnMgO system

The analysis of optical absorption spectra in the $(h\upsilon\alpha)^2 = f(h\upsilon)$ coordinates is presented in (*Figure 6*) which revealed a direct bandgap values. A direct bandgap of 3.37eV is found from the graph (*green line*). Bandgaps of 3.75 eV, 3.98 eV, and 4.31 eV are estimated for x value of 0.2 (*blue line*), 0.3 (*red line*), and 0.4 Mg (*black line*), respectively. The bandgap increases to 5.09 eV with increasing the x value to 0.6 (*purple line*). We suppose that the film with the x value of 0.6 has a mixed hexagonal-cubic crystal structure, since it is known that separation of phases occurs when the x value is in the range of $0.37 \leq x \leq 0.6$. A nearly linear increase of the bandgap with increasing the x value can be deduced from (*Figure 6b*).

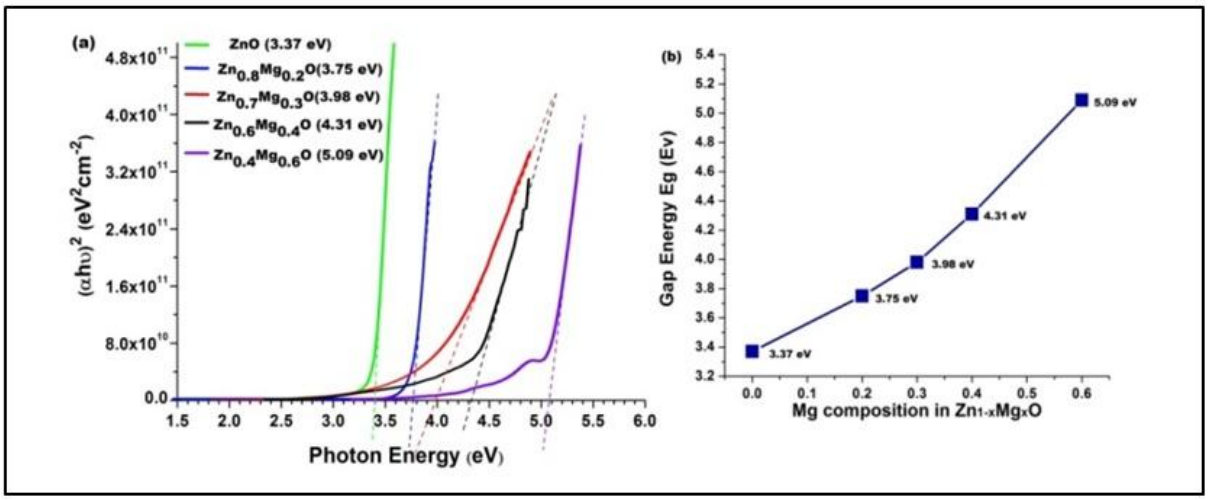

Figure 6. The analysis of optical absorption spectra of ZnO and $Zn_{1-x}Mg_xO$ films (a) and the dependence of the bandgap on the concentration of Mg (b).

Optical transmittance spectra of ZnO and ZnMgO thin films are compared in *(Figure 7)* depending on the photon energy. The transparency of the film with the higher concentration of Mg was approximately than 85% for x value of 0.4. The wavelength for ZnO is approximately 368 nm and by adding a higher concentration of Mg, we obtain the displacement of the emission spectrum up to 288 nm when x is 0.4.

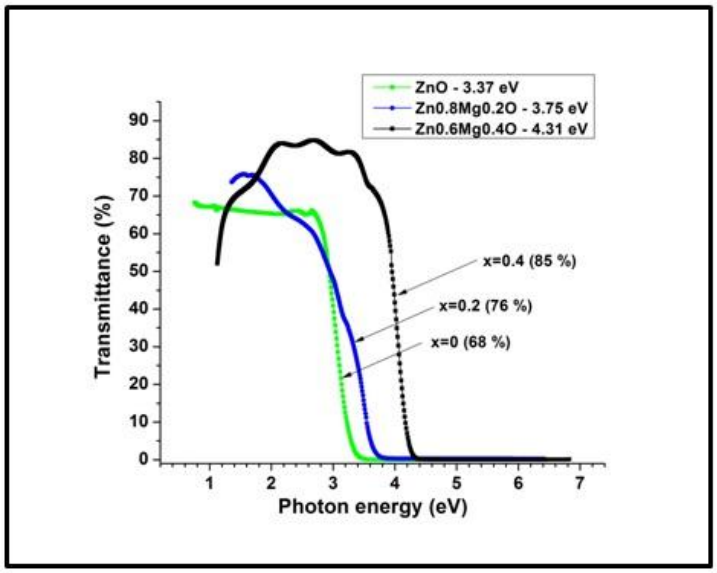

Figure 7. The analysis of optical transmittance spectrum of ZnO and $Zn_{1-x}Mg_xO$ films.

4. SUMMARY

We successfully deposited $Zn_{1-x}Mg_xO$ thin films with different concentration of Mg by the aerosol deposition method on Si substrates and demonstrated the photosensitivity functionality of these structures. It has been shown that as the concentration of Mg in ZnO increases, the band gap of the material increases. ZnMgO thin films are sensitive in a wide spectral range from ultraviolet (UV) to infrared (IR) radiation, with the highest sensitivity in the UV region.

5. ACKNOWLEDGEMENT

This work was supported financially by the National Agency for Research and Development of the Republic of Moldova under the grant no. 19.80013.50.07.02A/BL. VM thanks to the DAAD scholarships (German Academic Exchange Service) for support.

6. REFERENCES

[1] Y. N. Hou, Z. X. Meia, H. L. Liang, D. Q. Ye, C. Z. Gu, and X. L. Dua, "Dual-band MgZnO ultraviolet photodetector integrated with Si," Appl. Phys. Lett. 102, 153510 (2013).

[2] Shiau, J.-S.; Brahma, S.; Liu, C.-P.; Huang, J.-L, "Ultraviolet photodetectors based on MgZnO thin film grown by RF magnetron sputtering, "Thin Solid Films, 620, pp.170–174, (2016).

[3] Yang, J.-L.; Liu, K.-W.; Shen,D.-Z.Chin, "Recent progress of ZnMgO ultraviolet photodetector, " Chinese Physics B, 26, 047308, (2017).

[4] Kang, J.W.; Choi, Y.S.; Kim, B.H.; Kang, C.G.; Lee, B.H.; Tu, C.W.; Park, S.J, "Ultraviolet emission from a multi-layer graphene/MgZnO/ZnO light-emitting diode, " Appl. Phys. Lett., 104, 051120, (2014).

[5] Morshed, M.M.; Suja, M.; Zuo, M.Z.; Liu, J.L, "Ultraviolet random lasing from asymmetrically contacted MgZnO metal-semiconductor-metal device, " Appl. Phys. Lett., 105, 211107, (2014).

[6] Suja, M.; Bashar, S.B.; Debnath, B.; Su,L.; Shi, W.; Lake, R.; Liu, J, "Electrically driven deep ultraviolet MgZnO lasers at room temperature," Sci. Rep., 7, 2677, (2017).

[7] Z. G. Ju, C. X. Shan, D. Y. Jiang, J. Y. Zhang, B. Yao, D. X. Zhao, D. Z. Shenand X. W. Fan, "Mgx Zn1-x O basedphotodetectorscoveringthewholesolar-blindspectrumrange,"AppliedPhysicsLetters 93, 173505, (2008).

[8] D. C. Kim, B. Jung, J. H. Lee, H. K. Cho, J. Y. Lee and J. H. Lee, "Dramaticallyenhanced ultraviolet photosensing mechanism in a nanowires n-ZnO/i-MgO/n-Si structure with highly dense nanowires and ultrathin MgO layers,"Nanotechnology, pp.22 - 26, (2011).

[9] Ohmoto, A.; Kawasaki, M.; Koida, T.; Masubuchi, K.; Koinuma, H.; Sarukai, Y.; Yoshida, Y.; Yasuda, T.; Segawa, Y. MgxZn1−xO as a II–VI widegap semiconductor alloy. Appl. Phys. Lett., 72, 2466, (1998).

[10] Wang, X.; Saito, K.; Tanaka, T.;Nishio, M.; Nagaoka, T.; Arita, M.;Guo, Qi. A study on wide bandgap oxide semiconductors. Appl. Phys. Lett., 107, 022111, (2015).

[11] Toshihiko Maemoto, Nobuyasu Ichiba, Hiroaki Ishii, Shigehiko Sasa, and Masataka Inoue. Structural and optical properties of ZnMgO thin films grown by pulsed laser deposition using ZnO-MgO multiple targets. J. Phys.: Conf. Ser. 59, (2007).

[12] Lee, H.-Y.; Tsai, W.-H.; Lin, Y.-C.; Lee, C.-T. Diffusion barrier properties of transition metal thin films grown by plasma-enhanced atomic-layer deposition. Vac. Sci. Technol. B, 34, 051207, (2016).

[13] Maity, S.; Sahu, P.P.; Bhunia, C.T. High photo sensing performance with electrooptically efficient silicon based ZnO/ZnMgO heterojunction structure. IEEE Sensor., 18, pp. 6569– 6575, (2018).

[14] Chawla, S.; Jayanthi, K.; Chander, H. Enhancement of luminescence in ZnMgO thin-film nanophosphors and application for white light generation. Phys. Status Solidi A, 205, pp. 271–274, (2008).

[15] Hou, Y.N.; Mei, Z.X.; Liang, H.L.; Ye, D.Q.;Gu,C.Z.; Du,X.L. Dual-band MgZnO ultraviolet photodetector integrated with Si. Appl. Phys. Lett., 102, 153510, (2013).

[16] Morshed, M.M.; Suja, M.; Zuo, M.Z.; Liu, J.L. Ultraviolet random lasing from asymmetrically contacted MgZnO metal-semiconductor-metal device. Appl. Phys. Lett., 105, 211107, (2014).

[17] Liu, Z.L.; Mei, Z.X.; Wang, R.; Zhao, J.M.; Liang, H.L.; Guo, Y.; Kuznetsov, A. Yu.; Du, X.L. Alloy-fluctuation-induced exciton localization in high-Mg-content ($0.27 \leq x \leq 0.55$) wurtzite MgxZn1-xO epilayers. J. Phys. D: Appl. Phys., 43, 285402, (2010).

[18] Schoenfeld, W.V.; Wei, M.; Boutwell, R.C.; Liu, H.Y. High response solar-blind MgZnO photodetectors grown by molecular beam epitaxy. Proc. SPIE, 8987, 89871P, (2014).

[19] Thapa, D.; Huso, J.; Che, H.; Huso, M.; Morrison, M.; Gutierrez, D.; Grant Norton, M.; Bergman, L. Probing embedded structural inhomogeneities in MgZnO alloys via selective resonant Raman scattering. Appl. Phys. Lett., 102, 191902, (2013).

[20] Thapa, D.; Huso, J.;Miklos, K.; Wojcik, P.M.; McIlroy, D.N.; Morrison, J.L.; Corolewski, C.; McCluskey, M.D.; Williams, T.J.; Grant Norton, M.; Bergman, L. J. UV-luminescent MgZnO semiconductor alloys: nanostructure and optical properties. Mater. Sci.-Mater. El., 28, 2511-2520, (2017).

[21] Wu, C.-Z.; Ji,L.-W.; Liu, C.-H.; Peng, S.-M.; Young,S.-J.; Lam,K.-T.; Huang, C.-J. J. Ultraviolet photodetectors based on MgZnO thin films. Vac. Sci. Technol., A29, 03A118, (2011).

[22] Shiau, J.-S.; Brahma, S.; Liu, C.-P.; Huang, J.-L. Ultraviolet photodetectors based on MgZnO thin film grown by RF magnetron sputtering. Thin Solid Films, 620, pp.170–174, (2016).

[23] Kang, J.W.; Choi, Y.S.; Kim, B.H.; Kang, C.G.; Lee, B.H.; Tu, C.W.; Park, S. ZnO-Based Ultraviolet Light-Emitting Diode with a Graphene Transparent Hole Injection Layer. J. Appl. Phys. Lett., 104, 051120, (2014).

[24] Onuma, T.; Ono, M.; Ishii, K.; Kaneko, K.; Yamaguchi, T.; Fujita, S.; Honda, T. Impact of local arrangement of Mg and Zn atoms in rocksalt-structured MgxZn1−xO alloys on bandgap and deep UV cathodoluminescence peak energies. Appl. Phys. Lett., 113, 061903, (2018).

[25] Emanetoglu, N.W.; Muthukumar, S.; Wu, P.; Wittstruck, H.; Chen, Y.; Lu, Y. IEEE T. Ultrason. Ferr., 50, pp. 537-543, (2003).

[26] Wang, L.K.; Ju, Z.G.; Zhang, J.Y.; Zheng, J.; Shen, D.Z.; Yao, B.; Zhao, D.X.; Zhang, Z.Z.; Li, B.H.; Shan, C.X. Single-crystalline cubic MgZnO films and their application in deep-ultraviolet optoelectronic devices. Appl. Phys. Lett., 95, 131113, (2009).

[27] Lopez-Ponce, M.; Hierro, A.; Marin-Borras, V.; Tabares, G.; Kurtz, A.; Albert, S.; Agouram, S.; Munoz-Sanjose, V.; Munoz, E.; Ulloa, J. M. Optical properties of ZnMgO films grown by spray pyrolysis and their application to UV photodetection. Semicond. Sci. Tech., 30, 105026, (2015).

[28] Hierro, A.; Tabares, G.; Lopez-Ponce, M.;Ulloa, J.M.; Kurtz, A.; Munoz, E.; Marin-Borras, V.; Munoz-Sanjose, V.; Chauveau, J. ZnMgO-based UV photodiodes: a comparison of films grown by spray pyrolysis and MBE. M. Proc. SPIE, 9749, 97490W, (2016).

[29] Winkler ,N.; Edinger , S.; Kaur , J.; Wibowo, R.A.; Kautek , W.; Dimopoulos, T.; Solution-processed all-oxide solar cell based on electrodeposited Cu2O and ZnMgO by spray pyrolysis. J. Mater. Sci., 53, pp. 12231–12243, (2018).

[30] V. MORARI, V. POSTOLACHE, G. MIHAI, E. RUSU, ED. MONAICO, V. V. URSACHI, K. NIELSCH, AND I. M. TIGINYANU. Syntesis of $Mg_xZn_{1-x}O$ thin films by spin coating and aerosol deposition. In: The 9th ICMCS & The 6th CFM, Publications by Technical University of Moldova, Chișinău, October 19 – 21, pp. 483, (2017).

[31] Vadim MORARI, Aida PANTAZI, Nicolai CURMEI, Vitalie POSTOLACHE, Emil V. RUSU, Marius ENACHESCU, Ion M. TIGHINEANU and Veaceslav V. URSAKI. Band tail state related photoluminescence and photoresponse of ZnMgO solid solutions nanostructured films. Beilstein Journal Nanotechnology, Vol. 11, p. 899–910, (2020).

[32] Zhang, Q.; Gu, X.; Zhang, Q.; Jiang, J.; Jin, X.; Li, F.; Chen, Z.; Zhao, F.; Li, Q. ZnMgO:ZnO composite films for fast electron transport and high charge balance in quantum dot light emitting diodes. Opt. Mater. Express, 8, pp. 909-918, (2018).

[33] Singh, A.; Vij, A.; Kumar, D.; Khanna, P.K.; Kumar, M.; Gautam, S.; Chae, K.H. Investigation of phase segregation in sol–gel derived ZnMgO thin films. Semicond. Sci. Tech., 28, 025004, (2013).

[34] Tsay, C.-Y.; Chen, S.-T.; Fan, M.-T. Solution-Processed Mg-Substituted ZnO Thin Films for Metal-Semiconductor-Metal Visible-Blind Photodetectors. Coatings, 9 277, (2019).

[35] Chebil, W.; Boukadhaba, M.A.;Madhi, I.; Fouzri, A.; Lusson, A.; Vilar, C.; Sallet, V. Structural, optical and NO2 gas sensing properties of ZnMgO thin films prepared by the sol gel method. Physica B, 505, pp. 9-16, (2017).